

Massive neutrinos and degeneracies in Lyman-alpha forest simulations

Christian Pedersen,^a Andreu Font-Ribera,^a Thomas D. Kitching,^b Patrick McDonald,^c Simeon Bird,^d Anže Slosar,^e Keir K. Rogers,^f and Andrew Pontzen^a

^aDepartment of Physics and Astronomy, University College London, London, UK

^bMullard Space Science Laboratory, University College London, Dorking, Surrey, UK

^cLawrence Berkeley National Laboratory, One Cyclotron Road, Berkeley, CA 94720, USA

^dDepartment of Physics & Astronomy, University of California, Riverside, CA 92521, USA

^ePhysics Department, Brookhaven National Laboratory, Upton, NY 11973, USA

^fOskar Klein Centre for Cosmoparticle Physics, Stockholm University, AlbaNova, Stockholm SE-106 91, Sweden

E-mail: christian.pedersen.17@ucl.ac.uk

Abstract. Using a suite of hydrodynamical simulations with cold dark matter, baryons, and neutrinos, we present a detailed study of the effect of massive neutrinos on the 1-D and 3-D flux power spectra of the Lyman- α ($\text{Ly}\alpha$) forest. The presence of massive neutrinos in cosmology induces a scale- and time-dependent suppression of structure formation that is strongest on small scales. Measuring this suppression is a key method for inferring neutrino masses from cosmological data, and is one of the main goals of ongoing and future surveys like eBOSS, DES, LSST, Euclid or DESI. The clustering in the $\text{Ly}\alpha$ forest traces the quasi-linear power at late times and on small scales. In combination with observations of the cosmic microwave background, the forest therefore provides some of the tightest constraints on the sum of the neutrino masses. However there is a well-known degeneracy between Σm_ν and the amplitude of perturbations in the linear matter power spectrum. We study the corresponding degeneracy in the 1-D flux power spectrum of the $\text{Ly}\alpha$ forest, and for the first time also study this degeneracy in the 3-D flux power spectrum. We show that the non-linear effects of massive neutrinos on the $\text{Ly}\alpha$ forest, beyond the effect of linear power amplitude suppression, are negligible, and this degeneracy persists in the $\text{Ly}\alpha$ forest observables to a high precision. We discuss the implications of this degeneracy for choosing parametrisations of the $\text{Ly}\alpha$ forest for cosmological analysis.

Contents

1	Introduction	1
2	Linear theory	3
3	Simulations	5
4	Results	6
4.1	Non-linear growth of structure	7
4.2	Lyman- α forest clustering	9
5	Conclusion	11
A	Results at other redshifts	12
B	Dependence on box size and resolution	13
C	Dependence on neutrino implementation	14

1 Introduction

The results of neutrino oscillation experiments show that at least two of the neutrino mass eigenstates must have small but non-zero mass [1]. Whilst these experiments are able to constrain the mass differences of the eigenstates, they are far less sensitive to the absolute mass scale, or to the sum of the mass eigenstates Σm_ν . The extremely small cross section of neutrinos makes designing laboratory experiments to measure their absolute mass scale challenging. Attempts are continuing to be made through measuring the β -decay spectrum of tritium [2, 3], with the most recent results finding an upper limit of $\Sigma m_\nu < 1.1$ eV (90% C.L.) [4]. The subtle effects of neutrino properties on cosmology have been studied for decades [5, 6], and the onset of precision data sets in cosmology has opened up the possibility of measuring the neutrino mass scale by detecting the effect on the growth of structure and expansion rate of the Universe.

Constraints have been put on Σm_ν using several cosmological probes, such as observations of the CMB [7] or galaxy clustering and weak lensing measurements from galaxy surveys [8], and will continue to be a major science goal in future surveys [9]. Another cosmological probe that has emerged as an especially strong tool to constrain neutrino mass is the clustering of the Lyman- α (Ly α) forest: a series of absorption features observed in the spectra of high redshift ($2 < z < 5$) quasars. Some of the tightest constraints to date come from the combination of CMB and Ly α studies [10, 11], with a current limit of only $\Sigma m_\nu < 0.12$ eV (95% C.L.). With the upcoming Dark Energy Spectroscopic Instrument (DESI) survey constraints are forecast to shrink to $\sigma_{\Sigma m_\nu} = 0.041$ eV when utilising the full 3D power spectrum of the Ly α forest and combined with data from the CMB [12]. Given the current lower limit from oscillation experiments of $\Sigma m_\nu \geq 0.06$ eV, these observations should begin to show evidence for neutrino mass. When including information from the Ly α forest bispectrum the constraints could be further improved [13].

Three-dimensional correlations in the Ly α forest have been measured at separations of hundreds of Megaparsecs [14–17], allowing a very precise determination of the expansion rate at $z \approx 2.4$ from baryon acoustic oscillations. Most of the constraining power on total neutrino mass, however, comes from smaller separations as massive neutrino free-streaming suppresses clustering on small scales at late times. Current Ly α forest constraints on neutrino mass are restricted to the average correlation of one-dimensional Fourier modes along quasar spectra, a summary statistic commonly known as the 1D flux power spectrum.

In order to extract cosmological information from the measured correlations we need to be able to generate theoretical predictions for the flux power spectrum as a function of cosmological model and as a function of several nuisance parameters describing the uncertain thermal and ionization history of the intergalactic medium (IGM). In the absence of computing time constraints, one would run a large hydrodynamical simulation for each of the $10^5 - 10^6$ likelihood evaluations in a Monte Carlo Markov Chain. However, these simulations are computationally expensive, typically requiring $10^4 - 10^5$ core hours in high performance computing facilities, and past Ly α forest analyses were only able to simulate few tens of models. Some studies used the simulations to calibrate a Taylor expansion of the likelihood around a fiducial model [11, 18–21], while others designed different interpolation frameworks to predict the flux power spectrum for models that were not simulated [22]. Recent works have used Gaussian processes to perform this interpolation, which have the benefit of estimating an error on the prediction [23]. This allows for the use of Bayesian optimisation to distribute the hydrodynamical simulations more efficiently throughout parameter space, minimising the total number of simulations required and helping to ensure convergence to the true posterior distribution. [24].

The analysis is further complicated by the existence of several parameter degeneracies. For instance, both the mean transmitted flux fraction (or mean flux) and the amplitude of the linear power spectrum affect the overall amplitude of the 1D power spectrum of the Ly α forest, and we are only able to break the degeneracy because they affect its shape in a different way [22]. These degeneracies are difficult to capture in an interpolating framework or in a Taylor expansion, and numerical approximations might accidentally break these degeneracies in the estimated likelihood. Therefore it is important to choose a likelihood parameterization that minimizes the parameter degeneracies.

In this paper we investigate the degeneracy between the sum of the neutrino masses Σm_ν and the amplitude of the power spectrum. This degeneracy has been studied in the context of the matter power spectrum in real [25–27] and redshift space [28]. However, as discussed in [19], the degeneracy is stronger in studies of the 1D flux power spectrum of the Ly α forest, since it is primarily sensitive to the linear power on very small scales.

We revisit this degeneracy in the 1D flux power spectrum, with a different simulation set up to previous studies that captures the degeneracy more closely. For the first time we also study the degeneracy in the 3D flux power spectrum. In section 2 we review the effect of massive neutrinos in linear theory and discuss the parameter degeneracies. In section 3 we introduce a set of simulations to investigate how well the degeneracy predicted by linear theory carries over into the non-linear regime and into Ly α forest observables. Here we also describe the difference in our simulation set up when compared with previous studies into the degeneracy in the Ly α forest. In section 4 we present our results, and we conclude in section 5.

2 Linear theory

In this section we review the effect of massive neutrinos on the linear growth of structure (see [6] for a full review), focusing on effects on the linear power spectrum in the range of scales and redshifts relevant in studies of the small-scale clustering of the Ly α forest. We denote the density parameters defined at $z = 0$ for Cold Dark Matter (CDM), baryons, neutrinos, and dark energy as ω_c , ω_b , ω_ν and ω_Λ respectively. For each component, these are related to the critical density ρ_c via the density fractions $\Omega h^2 = \omega$ where $\Omega = \rho/\rho_c$. The total non-relativistic matter density at $z = 0$ is $\omega_{\text{cb}\nu} = \omega_c + \omega_b + \omega_\nu$.

The first effect of a non-zero neutrino mass is a subtle change in the expansion history of the Universe. At early times, massive neutrinos are relativistic and indistinguishable from massless ones, and their energy density decreases with the expansion of the universe like radiation. At late times, massive neutrinos become non-relativistic at redshift z_{nr} that is dependent on their mass, m_ν :

$$1 + z_{\text{nr}} = 189.4 \left(\frac{m_\nu}{0.1\text{eV}} \right). \quad (2.1)$$

From this point their energy density evolves like non-relativistic matter, and the total non-relativistic matter density is increased at the percent level:

$$f_\nu \equiv \frac{\omega_\nu}{\omega_{\text{cb}\nu}} = 0.023 \left(\frac{\Sigma m_\nu}{0.3 \text{ eV}} \right) \left(\frac{0.14}{\omega_{\text{cb}\nu}} \right), \quad (2.2)$$

where the neutrino energy density is given by

$$\omega_\nu = 0.00322 \left(\frac{\Sigma m_\nu}{0.3\text{eV}} \right). \quad (2.3)$$

After the non-relativistic transition neutrinos effectively behave like hot dark matter in that they free-stream and do not cluster on small scales. This length scale is set by the wavenumber which enters the horizon when neutrinos become non-relativistic:

$$k_{\text{nr}} \simeq 0.00213 \left(\frac{\omega_{\text{cb}\nu}}{0.14} \right)^{1/2} \left(\frac{m_\nu}{0.10\text{eV}} \right)^{1/2} \text{ Mpc}^{-1}, \quad (2.4)$$

This gives rise to the second effect of non-zero neutrino masses: the spatial distribution of CDM and baryons is affected by the distribution of neutrinos, as captured in the evolution of the linear power spectrum. In figure 1 we compare the linear power spectra¹ of CDM and baryons in a massless neutrino cosmology and a cosmology with three 0.1eV neutrinos. In this paper we assume that the Ly α forest is sensitive to the combined CDM and baryon power spectrum, and so we focus on this quantity rather than what is traditionally referred to as the matter power spectrum and includes massive neutrinos.

As can be seen in figure 1, the effect of massive neutrinos in the linear power spectrum is both redshift and scale-dependent. The scale dependence is set by the neutrino free-streaming scale (eq. 2.4), and we plot this as a vertical dashed line in figure 1. When comparing massive and massless neutrino cosmologies, there are several different choices one can make about which parameters to vary, and we show two options in the panels.

In the left panel we change ω_c to keep constant the total density of non-relativistic matter at low-redshift $\omega_{\text{cb}\nu}$. In the right panel we keep ω_c fixed and change the value of

¹Computed using the publicly available code CAMB[29]

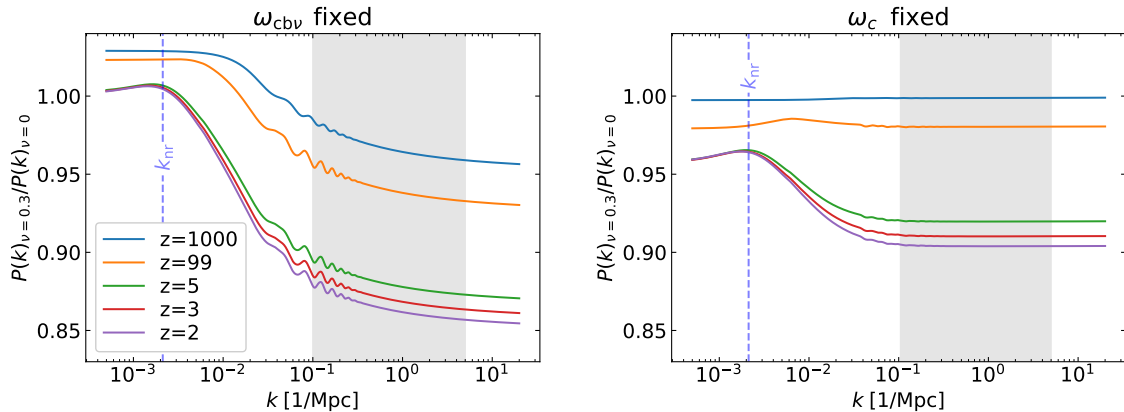


Figure 1. The effect of degenerate hierarchy $\Sigma m_\nu = 0.3\text{eV}$ massive neutrinos on the linear theory CDM + baryon power spectrum at several different redshifts, in two different scenarios: (left) ω_c is reduced to conserve the value of $\omega_{cb\nu}$ in both models; (right) ω_c , ω_b , and h are kept fixed, with the increase in $\omega_{cb\nu}$ when adding massive neutrinos compensated by reducing the value of ω_Λ in the model. The suppression on small scales due to massive neutrino free streaming is clear in both examples, however the small-scale suppression is only scale independent in the right panel. In blue dashed lines we show the neutrino free-streaming scale, k_{nr} , for a 0.1eV mass eigenstate, and the shaded area approximately represents the length scales probed by the one-dimensional flux power spectrum of the Ly α forest.

$\Omega_\Lambda = 1 - \Omega_{cb\nu}$. In both cases we keep fixed the baryon density parameter ω_b and the Hubble parameter h . In the left panel the effect at $z = 1000$ shown in blue is caused by the change in ω_c , as this is well before the neutrino relativistic transition ($z \gg z_{\text{nr}} = 188$). At low redshift, we see the characteristic suppression of power below the neutrino free-streaming scale ($k \gg k_{\text{nr}} = 0.0021 \text{ Mpc}^{-1}$). We note that the suppression has a mild scale- and redshift-dependence even on small scales ($k \approx 1 \text{ Mpc}^{-1}$).

When we keep ω_c fixed (right panel), adding a non-zero mass to neutrinos does not affect the physics of the early Universe ($z \gg z_{\text{nr}} = 188$), and the linear power at $z = 1000$ is practically unaffected. At much later times ($z \ll z_{\text{nr}} = 188$), and on scales smaller than the free-streaming scale, the effect of neutrinos is a scale-independent suppression of the linear power spectrum. Studies of the small-scale clustering of the Ly α forest are sensitive to the linear power in the approximate range shown shaded in gray in figure 1, which is well below the neutrino free-streaming scale. This suggests an almost perfect degeneracy in the linear power spectrum between the effect of massive neutrinos and the amplitude of the primordial power spectrum A_s when considering only these length scales, redshift ranges, and neutrino masses. For $\Sigma m_\nu > 0.5\text{eV}$ the suppression caused by neutrinos is no longer scale-independent at the lowest k modes probed by the Ly α forest, and so further work would be required to generalise the results presented in this paper for this neutrino mass range. We note that this threshold is higher than the current upper bound of $\Sigma m_\nu < 0.24\text{eV}$ from CMB measurements alone [7]. In the remaining sections of this paper we use hydrodynamical simulations to show that this degeneracy is also valid in the non-linear regime, and is still very strong in the Ly α flux power spectra.

3 Simulations

The simulations are run using the Tree-SPH code `MP-Gadget`², a modified version of `GADGET-2` [30] with the ability to simulate massive neutrinos and with an improved performance in massively parallelized runs [31].

Initial conditions for all our simulations were generated at $z = 99$, using separate, species specific, transfer functions for CDM and baryons computed using `CLASS` [32]. The CDM and baryon particles are both initialised on regular grids, offset to prevent particles being initialised at the same position. The initial conditions are generated using the Zel’dovich approximation at $z = 99$ with `MP-Gadget`’s inbuilt initial condition code, `MP-GenIC`. We do not use 2LPT because the terms have only been computed for a single initial fluid. The main results presented in this paper are from a set of simulations with box size $L = 133.85$ Mpc ($hL = 90$ Mpc), and 1024^3 CDM and baryon particles, and we show in appendix B that the conclusions of this paper do not depend on box size or resolution. In order to reduce cosmic variance, we use the ‘paired and fixed’ simulations introduced in [33, 34]. In this procedure, the initial amplitudes in each Fourier mode are fixed to the ensemble average instead of being randomly drawn, and for each cosmological model two simulations are run with the phases in each mode inverted. Clustering statistics such as the power spectrum are then taken to be the average of those calculated in each of the two simulations. To include the effects of reionisation, we use a uniform UV background following the model presented in ref. [35], which has been tuned to approximately match the observed IGM thermal history.

Including massive neutrinos in cosmological simulations presents its own set of technical challenges [36–40]. Neutrinos are often included as another species of particle in the simulation alongside the CDM and baryons [41–43]. However due to the comparatively low clustering of neutrino particles, especially for the lighter neutrino masses considered as the upper limit on Σm_ν becomes tighter, it is necessary to include a large number of neutrino particles in the simulation in order to reduce the shot noise below the level of the physical neutrino clustering [44]. This is in turn more computationally intensive, adding 50% to the walltime of a given simulation when using the same number of neutrino particles as CDM, as well as increasing memory and storage requirements.

An alternative approach was proposed in [45], which we refer to as the *Fourier space* approach, where the neutrino clustering is calculated using linear theory and then included in the gravitational potential used to evolve the baryon and CDM particles. This technique was further improved to a linear response in [46], where the linear evolution of the neutrino component is determined using the full non-linear density field of the CDM and baryon particles in the simulation. We use this implementation for the results presented in the main text of this paper, and demonstrate in appendix C that our findings do not depend on which approach is used. Unlike the particle implementation, the storage and memory requirements for massive neutrino simulations using the linear response approach are very similar to massless neutrino simulations, with a 5% increase in walltime with respect to the massless case that is largely independent of cosmological parameters.

The computation time of our simulations is significantly reduced by turning regions with gas density of $\rho_b/\bar{\rho}_b > 10^3$ directly into stars (`QuickLymanAlpha` option in `Gadget` simulations [47]), since these large overdensities do not affect the Ly α forest observables but are extremely computationally costly to evolve. The flux skewers are computed using `fake_spectra`³, which

²<https://github.com/MP-Gadget/MP-Gadget>

³https://github.com/sbird/fake_spectra

calculates the optical depth along a given line of sight. We compute the flux along a regular grid of 600^2 lines of sight at a cell resolution of 10km/s, providing high resolution both along and traverse to the line of sight. To calculate the 1D flux power spectrum, we take the Fourier transform of flux perturbations along each skewer, and then average each Fourier mode across all skewers in a given simulation. For the 3D flux power spectrum we utilise the fact that the skewers are calculated in an evenly spaced grid with the same line of sight resolution, and take a Fourier transform of flux perturbations for the entire box. The results are then averaged in bins of $k = |\vec{k}|$ and μ , where μ is the cosine of the angle of each Fourier mode with respect to the line of sight [48, 49].

In this study we run simulations for three different cosmologies: the *massive* simulation uses a cosmology with massive neutrinos ($\Sigma m_\nu = 0.3\text{eV}$); the *massless* simulation uses a similar cosmology but with massless neutrinos, resulting in a slightly lower $\omega_{\text{cb}\nu}$ at low redshift; the *rescaled* simulation uses the same cosmology as the *massless* simulation, but with a slightly lower amplitude of primordial fluctuations A_s . The value of A_s in the *rescaled* simulation is chosen in order to match the amplitude of the linear power spectrum of CDM + baryons in the *massive* simulation at a central redshift $z = 3$, and at a wavenumber⁴ $k = 0.7 \text{ Mpc}^{-1}$. Parameters for these simulations are shown in Table 1. The cosmology in the *massive* simulation has three neutrinos of degenerate hierarchy and $\Sigma m_\nu = 0.3\text{eV}$, which is slightly larger than the upper constraint provided by Planck alone [7]. We choose this extreme case as the idea we present will only become more reliable with lower values of Σm_ν .

The first detailed study into the degeneracy between the amplitude of the small scale linear power spectrum and Σm_ν in the context of the Ly α forest was presented in [19]. In our simulation set up we build upon this work, and intend to capture the degeneracy more completely with the following changes. Firstly, when adding massive neutrinos they kept the total matter content $\Omega_{\text{cb}\nu}$ fixed, which results in a slight scale dependence in the suppression even on small scales as seen in the left panel of figure 1 [19, 42]. The effect of this is that the linear theory power spectrum will not match on all length scales relevant for the Ly α forest. Secondly, in order to mimic the effect of massive neutrinos, they match σ_8 at $z = 7$, where σ_8 is calculated in each case from the total matter power spectrum including massive neutrinos. The Ly α forest is primarily sensitive to the clustering of the baryons and CDM rather than the clustering of the neutrinos themselves, and so we instead opt to match the CDM + baryon power spectrum at $z = 3$, neglecting the contribution from massive neutrinos. The suppression also has a slight redshift dependence, so fixing σ_8 at $z = 7$ would still result in imperfect agreement between the linear theory power spectra at lower redshifts where the Ly α forest is observed.

In the next section we compare the non-linear power spectra and Ly α forest observables for the simulations described in Table 1, and study to what degree the effects of massive neutrinos on these quantities can be replicated.

4 Results

In this section we present the results of our simulations. We examine how well the degeneracy in linear theory continues into the non-linear regime by looking at the matter power spectra in the three simulations described in Table 1. We then study the effect of massive neutrinos on the Ly α forest observables, the 1D and 3D flux power spectrum, as these are the key statistics that are ultimately used to constrain cosmology. As well as being dependent on

⁴The exact scale where we match the linear power is not important, see the right panel of figure 1.

	<i>massive</i>	<i>massless</i>	<i>rescaled</i>
Σm_ν (eV)	0.3	0.0	0.0
$\Omega_{\text{cb}\nu}$	0.3192	0.3121	0.3121
A_s	2.142e-9	2.142e-9	1.952e-9
Ω_c	0.2628		
Ω_b	0.0493		
n_s	0.9667		
h	0.6724		

Table 1. Simulations from which we obtain key results. We run three types of simulation: a simulation with $\Sigma m_\nu = 0.3\text{eV}$, a massless neutrino simulation, and a massless neutrino simulation where A_s has been rescaled in order to replicate the effect of massive neutrinos, referred to as a *rescaled* simulation. All cosmological parameters are kept constant except A_s , Σm_ν , and consequently $\Omega_{\text{cb}\nu}$.

the underlying non-linear power spectrum, the Ly α forest is also affected by the thermal and ionisation states of the IGM, which we will discuss in closer detail in section 4.2.

4.1 Non-linear growth of structure

First we look at the effect of massive neutrinos on the growth of structure in the non-linear regime, and examine to what extent these effects can be replicated simply by rescaling A_s . In figure 2 we plot the ratio of the CDM + baryon matter power spectra at $z = 3$ in our three cosmologies: The black line shows the linear theory result, also shown in the right panel of figure 1. The solid orange line compares the power in *massive* and *massless* simulations, where Ω_c and Ω_b are kept constant, and a $\Sigma m_\nu = 0.3\text{eV}$ neutrino mass has been added changing $\Omega_{\text{cb}\nu}$. We see the characteristic ‘spoon’ effect also seen in [19, 41] and references therein, which is because the onset of non-linearities are delayed as a result of the suppression of linear power.

The solid purple line shows the ratio of the power spectra in massive and massless neutrino cosmologies; however in this case we have rescaled the perturbation amplitude of the massless cosmology to match the small-scale linear power at $z = 3$ (*rescaled* cosmology in Table 1). The matter power spectrum at $z = 3$ in these two simulations agree to within 1% on all length scales relevant for Ly α forest analysis. We note that the star formation in these simulations is also extremely similar, with a difference of 0.05% at $z = 2$. The blue dashed line shows the ratio of the power spectra in the two massless cosmologies described in Table 1, that differ only in the value of A_s . In this case we see the same spoon effect as in the massive neutrino comparison, highlighting the fact that this feature is a consequence of the suppression of structure growth on linear scales and can be replicated without massive neutrinos.

If the Ly α forest power spectrum were measured at a single redshift, this would be sufficient: the solid purple line in figure 2 shows that the effect of massive neutrinos can be reproduced to sub-percent agreement by a rescaling of the amplitude of initial perturbations. However, in the right panel of figure 1 we see that the effect of massive neutrinos on the small scale linear power has a redshift dependence, varying by a couple of percent over the redshift range covered by the Ly α forest, $5 > z > 2$, meaning that rescaling A_s will only match the linear power perfectly at a single redshift.

To investigate this effect we pick two modes, one linear ($k_L = 0.3 \text{ Mpc}^{-1}$) and one non-linear ($k_{\text{NL}} = 3 \text{ Mpc}^{-1}$). In the purple lines of figure 3, we plot the ratio of the power in these

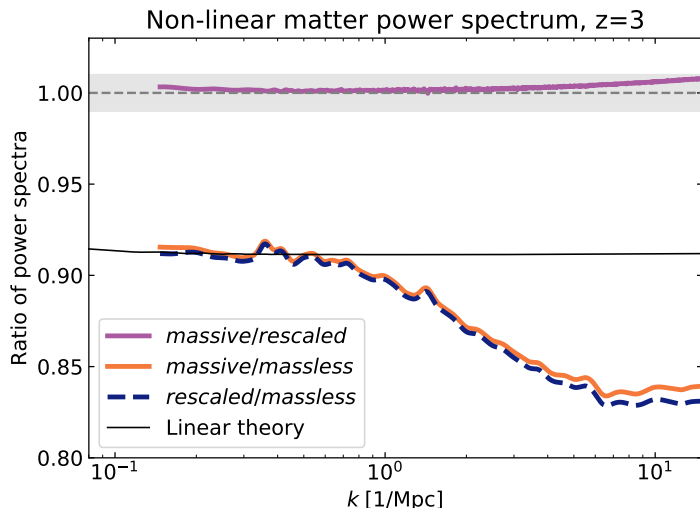


Figure 2. The ratio of the matter power spectra (CDM+baryons) in simulations with massive and massless neutrinos. The black line shows the linear theory result for the cosmologies in the *massive* and *massless* simulations described in Table 1, which is the same as the red line in figure 1 right panel. The solid orange line shows a comparison between the full non-linear matter power spectra in the *massive* and *massless* simulations. The solid purple line represents the comparison between the *massive* and *rescaled* cosmology, a massless neutrino cosmology with a lower clustering amplitude A_s to match the small-scale linear power at $z = 3$. In dashed blue, we compare the two massless neutrino cosmologies, showing that the ‘spoon’ effect can be recreated without any massive neutrinos. The gray band shows the region of 1% agreement.

modes in the *massive* and *rescaled* simulations, with the ratio for k_L shown in solid lines, and k_{NL} shown in dashed lines. By construction the amplitude in the linear mode is matched at $z = 3$, but due to the different growth rates in the two cosmologies, there are disagreements at the percent level at $z = 5$ and $z = 2$. We note that this is a very small effect that is still well below the precision of current measurements of the amplitude of the linear power from the Ly α forest which are on the order of 10% [22, 50]. This effect is also very small when compared with the size of the suppression caused by massive neutrinos, which is 9% for our case of $\Sigma m_\nu = 0.3$.

In the green lines we plot the same ratios, except where we have output the snapshots in the *rescaled* simulation at a slightly different redshift in order to match the amplitude of the linear power. For instance, we compare the snapshot at $z = 5$ for the *massless* simulation with a snapshot of the *rescaled* simulation at $z = 4.97$. While the ratio of the power in the linear modes changes as a function of redshift in the purple lines, it is constant in the green lines. When matching the amplitude of the power in the linear mode, the power in the non-linear mode agrees to within 0.5% across the full redshift range, even when massive neutrinos are not included in the simulation. This tells us again that the non-linear structure is primarily sensitive to the amplitude in the linear power, and that any non-linear effects caused by massive neutrinos themselves are negligible with respect to current precision.

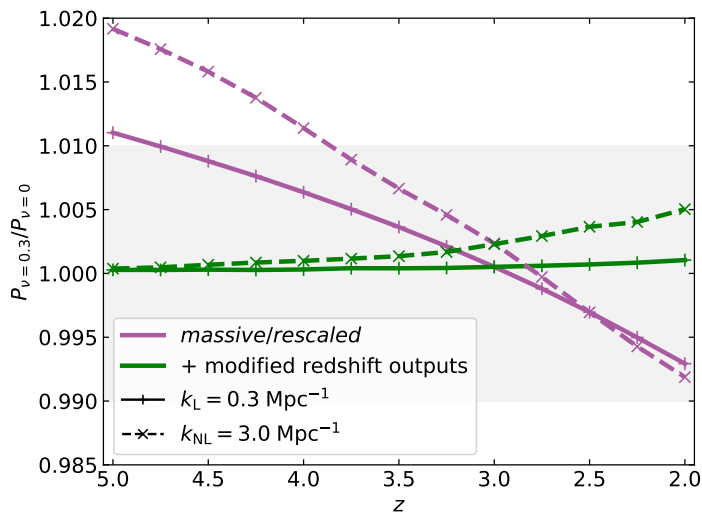


Figure 3. The ratios of the matter power spectra in the *massive* and *rescaled* simulations for a linear (solid lines) and non-linear (dashed) mode across the full redshift range $5 > z > 2$. In purple lines, the ratio has a small redshift dependence due to the fact that the growth in the two cosmologies is different. By design, the ratios in the linear modes are matched at $z = 3$. In green lines, we have modified the redshifts at which snapshots are output to match the linear power in the two simulations. When the linear power is matched, the power in the non-linear mode agrees to within 0.5%.

4.2 Lyman- α forest clustering

In this section we look at the statistics of the Ly α forest, and examine the degeneracy between massive neutrinos and the amplitude of primordial fluctuations. In particular, we look at correlations of the fluctuating transmitted flux fraction, $\delta_F(\mathbf{x}) = F(\mathbf{x})/\bar{F} - 1$, where \bar{F} is the mean transmitted flux fraction. In principle, one could measure the full 3D power spectrum,

$$\langle \delta_F(\mathbf{k}) \delta_F(\mathbf{k}') \rangle = (2\pi)^3 \delta^D(\mathbf{k} + \mathbf{k}') P_{3D}(k, \mu) \quad (4.1)$$

where $\delta_F(\mathbf{k})$ is the Fourier transform of $\delta_F(\mathbf{x})$ and μ is the cosine of the angle between the Fourier mode and the line-of-sight, and use it to constrain cosmology [51]. However, current Ly α constraints on neutrino mass use exclusively the 1D power spectrum,

$$P_{1D}(k_{\parallel}) = \int_0^{\infty} \frac{dk_{\perp} k_{\perp}}{2\pi} P_{3D}(k_{\perp}, k_{\parallel}), \quad (4.2)$$

where k_{\parallel} and k_{\perp} are the components of the Fourier mode along and perpendicular to the line of sight respectively, $k_{\parallel} = k\mu$, and $k^2 = k_{\parallel}^2 + k_{\perp}^2$.

The 1D and 3D flux power spectra of the Ly α forest are dependent on both the matter density field and the state of the IGM, and there is also some dependence on the velocity power spectrum through redshift space distortions. Due to the different initial conditions, the IGM history in the *massive* and *rescaled* simulations is different, which will propagate to differences in the flux power spectra. However these differences do not mean that the degeneracy shown in figures 2 and 3 is broken as the state of the IGM is marginalised over in cosmological analysis of the Ly α forest due to uncertainties in the astrophysics of reionisation. These subtle changes in the state of the IGM therefore cannot be interpreted as signatures of

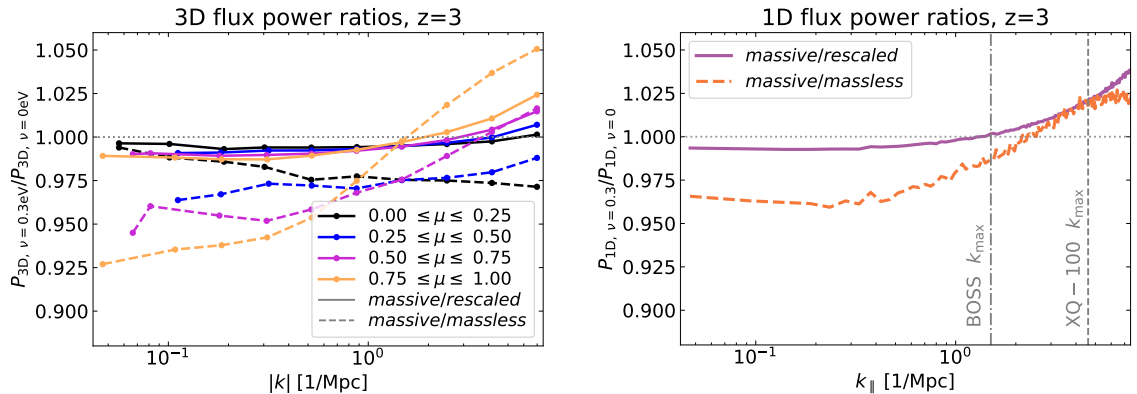


Figure 4. *Left:* Ratios of the 3D flux power spectra in simulations with and without massive neutrinos as a function of 3D Fourier mode orientation μ . Dashed lines show the ratios for the *massless* simulation, while solid lines show the ratios for the *rescaled* simulation. In both cases, T_0 and the mean flux have been matched in each simulation pair. *Right:* Ratios of 1D flux power spectra in massive and massless neutrino cosmologies. The ratio for the *massless* simulation is shown in orange dashed lines and the ratio for the *rescaled* simulation in purple solid lines. In the gray dot-dashed line we show the highest k_{\parallel} bin measured in BOSS data [54], and in gray dashed we show the we show k_{max} for higher resolution data [55].

massive neutrinos. Given imperfect parametrisations of the IGM and the highly non-linear relationship between these parameters and the observable flux power spectra, it is impossible to isolate all of these effects and match them by hand in the way that we have done with the linear power.

A full marginalization is beyond the scope of this paper, but we match two of the IGM parameters – the mean flux and the temperature at mean density in the simulations – to remove some effects of neutrinos that are degenerate with nuisance parameters. The temperature of the gas in the IGM is well approximated by a power-law distribution of the form $T(\delta_b) = T_0(1 + \delta_b)^{\gamma-1}$ where δ_b is the baryon overdensity, and T_0 is the temperature at mean density [52]. Given that the power-law approximation only holds at low densities, we perform the fit in the range $-2 < \log_{10}(\delta_b) < 0.5$. This is appropriate given that these overdensities are also the regions which give rise to the Ly α forest [53]. We match the mean flux by re-scaling the optical depth in the skewers by a constant in post-processing. We also match T_0 in the simulations. For the heavily ionised gas in photoionisation equilibrium which gives rise to the Ly α forest the gas temperature is proportional to the internal energy. This allows us to rescale the temperature at mean density in the simulations by a constant rescaling of the internal energies of the particles, as long as the rescalings are small. In both cases the rescalings were small, on the order of 2%.

In figure 4 we look at the effect of massive neutrinos on the flux power spectra after recalibrating \bar{F} and T_0 as described above, and study the degeneracy with the amplitude of the linear power. The left panel shows the ratios of the 3D flux power spectra in simulations with and without massive neutrinos. The dashed lines show the comparison between the *massive* and *massless* simulations. There is a significant difference between the flux power spectra in these two simulations, particularly along the line of sight, with $\mu \sim 1$. The solid lines show that the majority of this difference comes from the difference in the amplitude of

the linear power, as the difference in the flux power spectra shrinks to $\lesssim 1\%$ for $k < 4 \text{ Mpc}^{-1}$ once the amplitude of the linear power is matched. In particular for modes transverse to the line of sight (shown in black) there is a near perfect match. The high k modes along the line of sight still show some deviation, which is suggesting some residual difference in the thermal state of the IGM. Additionally there is a signature of neutrinos that is not captured in the matter power spectrum but does affect the flux power spectrum, which comes from the change in the growth rate. As discussed in section 4.1, the presence of massive neutrinos causes a 2% difference in the growth rate, which has an effect on the flux power spectrum through a change in the gas velocities. This is a feature of massive neutrinos that we do not account for in our current setup, but the results in figure 4 indicate that the effect is very small.

The right panel shows the ratios of the 1D flux power spectra for the same simulations, where the orange dashed line is the ratio of the *massless* and *massive* simulations, and the purple solid line is the ratio of the *massive* and *rescaled*. The vertical gray dashed lines show the highest k_{\parallel} modes that have been used in recent cosmological analysis. The purple solid line shows that the effects of massive neutrinos can be replicated by rescaling the linear power to within at least 1% on scales measured by BOSS, and within 2.5% for the higher resolution data⁵.

Upcoming measurements from DESI are not expected to increase to significantly higher values of k_{\parallel} , but the improvement in the data will come from a more precise measurement of the same k_{\parallel} range. Therefore the results that we present in this paper will still be applicable for analysing DESI datasets. We reiterate that our approach of matching the mean flux and T_0 does not fully explore the degeneracy. For example, the optimum match of the ratios shown in figure 4 might be for IGM values that are not the same in each simulation, i.e. \bar{F} and T_0 could be tweaked to push the ratios closer to 1. What will ultimately matter is to what extent the effects of Σm_{ν} are degenerate with a change in these nuisance parameters, which would require a full marginalisation.

While the results in figure 4 are shown only at $z = 3$, in appendix A we show the equivalent plots for other redshifts and note that the results are largely independent of redshift. Together these results indicate a strong degeneracy between A_s and Σm_{ν} when considering only the length scales and redshift ranges that are observed using the Ly α forest.

5 Conclusion

We have considered the effects of massive neutrinos on the growth of structure within the length scales and redshift range relevant for Ly α forest analysis. These effects can be split into three categories. First there is a suppression of the overall amplitude of the power spectrum. Second there is an increase in the non-linear growth caused by the presence and clustering of massive neutrinos. Third there is an effect on the growth rate and velocity power spectrum. The first effect is large, with a 9% suppression of the power spectrum for $\Sigma m_{\nu} = 0.3 \text{ eV}$. The Ly α forest is sensitive to the amplitude of the late-time, small scale power spectrum, and so this is the strongest signal of neutrino mass when using Ly α forest data. However we have shown that this signal is extremely degenerate with a change in the primordial perturbation amplitude, A_s . In section 4.1 we showed that even non-linear effects caused by massive neutrinos are also highly degenerate with a change in the overall amplitude of the power spectrum.

⁵Note that the 10km/s skewer resolution is low compared with high resolution spectra e.g. [55]. We therefore verified that our results are unchanged when adopting 5 km/s skewers.

In figure 3 we showed that the effect of massive neutrinos on the growth rate is small, with a $< 2\%$ effect on the non-linear modes. The Ly α forest is far less sensitive to the growth rate - Ref [22] measured the growth rate to a precision of 30%, while the amplitude of the linear power was measured to a precision of 13% - and so we argue that effects on the growth rate do not break the degeneracy with A_s . We demonstrated this degeneracy on the flux power spectra of the Ly α forest and showed that, after matching the mean flux and temperature at mean density, the effect of $\Sigma m_\nu = 0.3$ eV massive neutrinos is degenerate with A_s to within $< 1\%$ in the 1D flux power at $k_{\parallel} < 3 \text{ Mpc}^{-1}$ and in the 3D flux power at $|k| < 4 \text{ Mpc}^{-1}$.

Therefore, from the point of view of a Ly α forest only likelihood, we have shown that it is not necessary to include an extra parameter to describe neutrino mass, and that doing so introduces a strong degeneracy. An interesting future work would be to investigate to what extent this degeneracy persists into higher order statistics. Our results also suggest that other parametrisations based on the amplitude of the linear power at low z and high k would more closely describe the observables, but we leave the exact specification of such parametrisations for future work. We finish by stressing that, even in the presence of this degeneracy, the Ly α forest is still a very competitive probe of massive neutrinos when combined with results from CMB experiments. The CMB temperature fluctuations depend on the linear power spectrum at early times, before neutrinos become non-relativistic, and provide a measurement of A_s that can be used to break the $A_s - \Sigma m_\nu$ degeneracy discussed in this work. We expect that combined CMB + Ly α forest analyses will continue to play an important role in cosmological studies of neutrino masses in the coming years.

Acknowledgments

The authors thank the organisers and participants of the IGM2018 conference at Kavli IPMU for hosting valuable discussions. We thank Yu Feng for assistance in running `MP-Gadget`. This work was partially enabled by funding from the UCL Cosmoparticle Initiative. This work was supported by collaborative visits funded by the Cosmology and Astroparticle Student and Postdoc Exchange Network (CASPEN). AFR acknowledges support by an STFC Ernest Rutherford Fellowship, grant reference ST/N003853/1. AFR and AP were further supported by STFC Consolidated Grant number ST/R000476/1. TDK and AP are supported by a Royal Society University Research Fellowship. SB was supported by NSF grant AST-1817256. KKR was supported by the Science Research Council (VR) of Sweden. This work was performed using the Cambridge Service for Data Driven Discovery (CSD3), part of which is operated by the University of Cambridge Research Computing on behalf of the STFC DiRAC HPC Facility (www.dirac.ac.uk). The DiRAC component of CSD3 was funded by BEIS capital funding via STFC capital grants ST/P002307/1 and ST/R002452/1 and STFC operations grant ST/R00689X/1. DiRAC is part of the National e-Infrastructure.

A Results at other redshifts

In figure 5 we show the ratios of both the 1D and 3D flux power spectra for the *massive* and *rescaled* simulations at redshifts $z = 4.5, 3.5, 2$. We have matched the mean flux and temperature at mean density. The ratios of the 1D and 3D flux power spectra have essentially the same amplitude and shape as the $z = 3$ ratios presented in section 4.2. This shows that over the full redshift range relevant for Ly α forest the flux power spectrum is primarily dependent on the amplitude of the linear power and the state of the IGM, and the effects of massive neutrinos can be replicated to within 2% by matching these parameters.

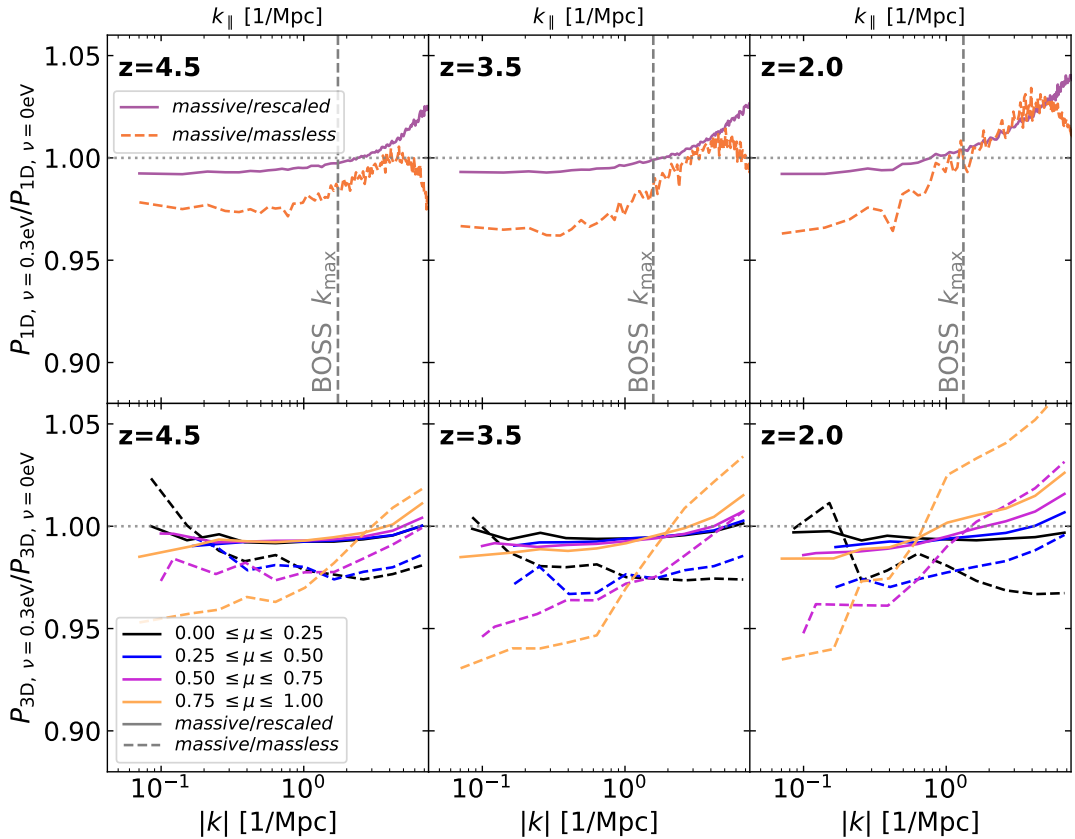


Figure 5. Ratios of 1D (top) and 3D (bottom) flux power spectra in simulations with massive and massless neutrinos, at different redshifts. In both panels, the solid lines show the ratios of the flux power spectra in the *massive* simulation and the *rescaled*, the ratios for the *massive* and *massless* simulation are shown in dashed lines. The mean flux and the temperature at mean density have been matched in both simulations to reduce the effect of subtle changes in the thermal and ionization history of the IGM. In vertical lines we show the highest k mode measured from BOSS data in [54] for each redshift bin.

B Dependence on box size and resolution

In section 4 we have presented the results from a set of simulations with a box size of $L = 133.85$ Mpc ($hL = 90$ Mpc), and 1024^3 CDM and baryon particles. In order to test that the main results do not depend on the chosen box size or resolution, in figure 6 we reproduce the results of the left panel in figure 4 from simulations with $L = 89.23$ Mpc ($hL = 60$ Mpc), and 512^3 CDM and baryon particles. The original results from the main text are shown in solid lines, and the dashed lines show the results from the simulation with lower box size and lower resolution. There is very little difference between the results shown in the solid and dashed lines, indicating that the results shown in section 4.2 are independent of simulation box size and resolution.

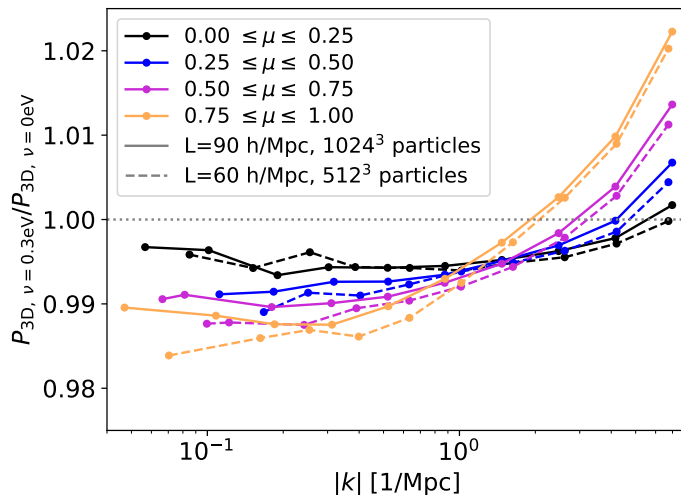


Figure 6. Ratios of the 3D flux power spectra in the *massive* and *rescaled* cosmologies at $z = 3$ for two different sets of simulations; one with box sizes of $L = 90 h^{-1}\text{Mpc}$ and 1024^3 particles (solid lines), and one with box sizes of $L = 60 h^{-1}\text{Mpc}$ and 512^3 particles (dashed lines). We have matched \bar{F} and T_0 in each simulation pair. The results presented in section 4.2 are independent of box size and resolution.

C Dependence on neutrino implementation

In order to verify that our results are independent of neutrino implementation, we show in figure 7 the ratio of power spectra at $z = 2$ in simulations with the linear response approximation and particle neutrinos. We include the same number of neutrino particles as CDM and baryons ($N_{\text{part}} = 512^3$), with initial conditions also starting at $z = 99$. The particle implementation can include (small) non-linear clustering in the neutrino component, whereas the Fourier space approach only includes non-linearities in the cold dark matter. We show the comparison at the lowest redshift we have run simulations to as this is where any disagreement between the two methods would be strongest. For the CDM + baryon density (left), 1D (center) and 3D (right) flux power spectra, the agreement between the two approaches is better than 0.5%. This is consistent with the expectation that there is minimal non-linear clustering of neutrinos at $z = 2$ (see refs [41, 46]), and the residual difference is likely due to shot noise in the neutrino particles. A similar comparison at other redshifts can be found in figures 5 and 7 of ref [46].

References

- [1] P. F. de Salas, D. V. Forero, C. A. Ternes, M. Tortola and J. W. F. Valle, *Status of neutrino oscillations 2018: first hint for normal mass ordering and improved CP sensitivity*, *arXiv e-prints* (2017) [[1708.01186](#)].
- [2] C. Kraus, L. Bornschein, J. Bonn, B. Bornschein, B. Flatt, A. Kovalik et al., *The Mainz Neutrino Mass Experiment*, *Nuclear Physics B Proceedings Supplements* **143** (2005) 499.
- [3] K. Eitel, *Direct Neutrino Mass Experiments*, *Nuclear Physics B Proceedings Supplements* **143** (2005) 197.

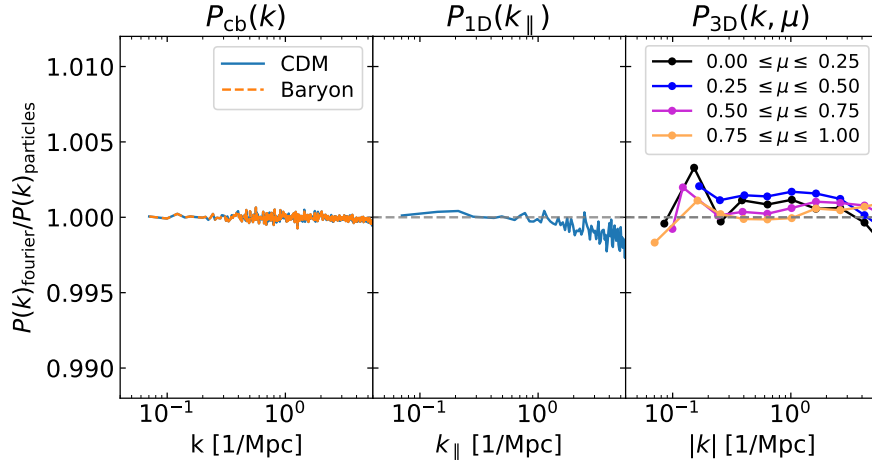


Figure 7. Comparison of the Fourier space based neutrinos with the particle implementation at $z = 2$. From left to right, we show the ratios of the CDM + baryon matter power spectra, the 1D flux power and then the 3D flux power spectra.

- [4] M. Aker, K. Altenmüller, M. Arenz, M. Babutzka, J. Barrett, S. Bauer et al., *An improved upper limit on the neutrino mass from a direct kinematic method by KATRIN*, *arXiv e-prints* (2019) arXiv:1909.06048 [[1909.06048](#)].
- [5] J. R. Bond, G. Efstathiou and J. Silk, *Massive neutrinos and the large-scale structure of the universe*, *Phys. Rev. Lett.* **45** (1980) 1980.
- [6] J. Lesgourgues and S. Pastor, *Massive neutrinos and cosmology*, *Phys. Rept.* **429** (2006) 307 [[astro-ph/0603494](#)].
- [7] Planck Collaboration, N. Aghanim, Y. Akrami, M. Ashdown, J. Aumont, C. Baccigalupi et al., *Planck 2018 results. VI. Cosmological parameters*, *ArXiv e-prints* (2018) arXiv:1807.06209 [[1807.06209](#)].
- [8] T. M. C. Abbott, F. B. Abdalla, A. Alarcon, J. Aleksić, S. Allam, S. Allen et al., *Dark Energy Survey year 1 results: Cosmological constraints from galaxy clustering and weak lensing*, *Phys. Rev. D* **98** (2018) 043526 [[1708.01530](#)].
- [9] J. Hamann, S. Hannestad and Y. Y. Y. Wong, *Measuring neutrino masses with a future galaxy survey*, *JCAP* **2012** (2012) 052 [[1209.1043](#)].
- [10] U. Seljak, A. Slosar and P. McDonald, *Cosmological parameters from combining the Lyman- α forest with CMB, galaxy clustering and SN constraints*, *Journal of Cosmology and Astro-Particle Physics* **2006** (2006) 014 [[astro-ph/0604335](#)].
- [11] N. Palanque-Delabrouille, C. Yèche, J. Baur, C. Magneville, G. Rossi, J. Lesgourgues et al., *Neutrino masses and cosmology with Lyman-alpha forest power spectrum*, *JCAP* **2015** (2015) 011 [[1506.05976](#)].
- [12] A. Font-Ribera, P. McDonald, N. Mostek, B. A. Reid, H.-J. Seo and A. Slosar, *DESI and other Dark Energy experiments in the era of neutrino mass measurements*, *Journal of Cosmology and Astro-Particle Physics* **2014** (2014) 023 [[1308.4164](#)].
- [13] R. Mandelbaum, P. McDonald, U. Seljak and R. Cen, *Precision cosmology from the Lyman α forest: power spectrum and bispectrum*, *Mon. Not. Roy. Astron. Soc.* **344** (2003) 776 [[astro-ph/0302112](#)].

- [14] N. G. Busca, T. Delubac, J. Rich, S. Bailey, A. Font-Ribera, D. Kirkby et al., *Baryon acoustic oscillations in the Ly α forest of BOSS quasars*, *Astron. Astrophys.* **552** (2013) A96 [[1211.2616](#)].
- [15] A. Slosar, V. Iršič, D. Kirkby, S. Bailey, N. G. Busca, T. Delubac et al., *Measurement of baryon acoustic oscillations in the Lyman- α forest fluctuations in BOSS data release 9*, *Journal of Cosmology and Astro-Particle Physics* **2013** (2013) 026 [[1301.3459](#)].
- [16] T. Delubac, J. E. Bautista, N. G. Busca, J. Rich, D. Kirkby, S. Bailey et al., *Baryon acoustic oscillations in the Ly α forest of BOSS DR11 quasars*, *Astron. Astrophys.* **574** (2015) A59 [[1404.1801](#)].
- [17] J. E. Bautista, N. G. Busca, J. Guy, J. Rich, M. Blomqvist, H. du Mas des Bourboux et al., *Measurement of baryon acoustic oscillation correlations at $z = 2.3$ with SDSS DR12 Ly α -Forests*, *Astron. Astrophys.* **603** (2017) A12 [[1702.00176](#)].
- [18] M. Viel and M. G. Haehnelt, *Cosmological and astrophysical parameters from the Sloan Digital Sky Survey flux power spectrum and hydrodynamical simulations of the Lyman α forest*, *Mon. Not. Roy. Astron. Soc.* **365** (2006) 231 [[astro-ph/0508177](#)].
- [19] M. Viel, M. G. Haehnelt and V. Springel, *The effect of neutrinos on the matter distribution as probed by the intergalactic medium*, *Journal of Cosmology and Astro-Particle Physics* **2010** (2010) 015 [[1003.2422](#)].
- [20] A. Borde, N. Palanque-Delabrouille, G. Rossi, M. Viel, J. S. Bolton, C. Yèche et al., *New approach for precise computation of Lyman- α forest power spectrum with hydrodynamical simulations*, *Journal of Cosmology and Astro-Particle Physics* **2014** (2014) 005 [[1401.6472](#)].
- [21] G. Rossi, N. Palanque-Delabrouille, A. Borde, M. Viel, C. Yèche, J. S. Bolton et al., *Suite of hydrodynamical simulations for the Lyman- α forest with massive neutrinos*, *Astron. Astrophys.* **567** (2014) A79 [[1401.6464](#)].
- [22] P. McDonald, U. Seljak, R. Cen, D. Shih, D. H. Weinberg, S. Burles et al., *The Linear Theory Power Spectrum from the Ly α Forest in the Sloan Digital Sky Survey*, *ApJ* **635** (2005) 761 [[astro-ph/0407377](#)].
- [23] S. Bird, K. K. Rogers, H. V. Peiris, L. Verde, A. Font-Ribera and A. Pontzen, *An emulator for the Lyman- α forest*, *Journal of Cosmology and Astro-Particle Physics* **2019** (2019) 050 [[1812.04654](#)].
- [24] K. K. Rogers, H. V. Peiris, A. Pontzen, S. Bird, L. Verde and A. Font-Ribera, *Bayesian emulator optimisation for cosmology: application to the Lyman-alpha forest*, *Journal of Cosmology and Astro-Particle Physics* **2019** (2019) 031 [[1812.04631](#)].
- [25] F. Villaescusa-Navarro, F. Marulli, M. Viel, E. Branchini, E. Castorina, E. Sefusatti et al., *Cosmology with massive neutrinos I: towards a realistic modeling of the relation between matter, haloes and galaxies*, *JCAP* **2014** (2014) 011 [[1311.0866](#)].
- [26] M. Zennaro, R. E. Angulo, G. Aricò, S. Contreras and M. Pellejero-Ibáñez, *How to add massive neutrinos to your Λ CDM simulation - extending cosmology rescaling algorithms*, *Mon. Not. Roy. Astron. Soc.* **489** (2019) 5938 [[1905.08696](#)].
- [27] M. Archidiacono, T. Brinckmann, J. Lesgourgues and V. Poulin, *Physical effects involved in the measurements of neutrino masses with future cosmological data*, *JCAP* **2017** (2017) 052 [[1610.09852](#)].
- [28] F. Villaescusa-Navarro, A. Banerjee, N. Dalal, E. Castorina, R. Scoccimarro, R. Angulo et al., *The Imprint of Neutrinos on Clustering in Redshift Space*, *ApJ* **861** (2018) 53 [[1708.01154](#)].
- [29] A. Lewis, A. Challinor and A. Lasenby, *Efficient Computation of Cosmic Microwave Background Anisotropies in Closed Friedmann-Robertson-Walker Models*, *ApJ* **538** (2000) 473 [[astro-ph/9911177](#)].

- [30] V. Springel, *The cosmological simulation code GADGET-2*, *Mon. Not. Roy. Astron. Soc.* **364** (2005) 1105 [[astro-ph/0505010](#)].
- [31] Y. Feng, S. Bird, L. Anderson, A. Font-Ribera and C. Pedersen, *Mp-gadget/mp-gadget: A tag for getting a doi*, Oct., 2018. 10.5281/zenodo.1451799.
- [32] J. Lesgourgues, *The Cosmic Linear Anisotropy Solving System (CLASS) I: Overview*, *arXiv e-prints* (2011) arXiv:1104.2932 [[1104.2932](#)].
- [33] R. E. Angulo and A. Pontzen, *Cosmological N-body simulations with suppressed variance*, *Mon. Not. Roy. Astron. Soc.* **462** (2016) L1 [[1603.05253](#)].
- [34] L. Anderson, A. Pontzen, A. Font-Ribera, F. Villaescusa-Navarro, K. K. Rogers and S. Genel, *Cosmological Hydrodynamic Simulations with Suppressed Variance in the Lyman- α Forest Power Spectrum*, *arXiv e-prints* (2018) arXiv:1811.00043 [[1811.00043](#)].
- [35] E. Puchwein, F. Haardt, M. G. Haehnelt and P. Madau, *Consistent modelling of the meta-galactic UV background and the thermal/ionization history of the intergalactic medium*, *Mon. Not. Roy. Astron. Soc.* **485** (2019) 47 [[1801.04931](#)].
- [36] S. Hannestad, T. Haugbølle and C. Schultz, *Neutrinos in non-linear structure formation — a simple SPH approach*, *JCAP* **2012** (2012) 045 [[1110.1257](#)].
- [37] A. Banerjee and N. Dalal, *Simulating nonlinear cosmological structure formation with massive neutrinos*, *JCAP* **2016** (2016) 015 [[1606.06167](#)].
- [38] J. D. Emberson, H.-R. Yu, D. Inman, T.-J. Zhang, U.-L. Pen, J. Harnois-Déraps et al., *Cosmological neutrino simulations at extreme scale*, *Research in Astronomy and Astrophysics* **17** (2017) 085 [[1611.01545](#)].
- [39] S. Bird, Y. Ali-Haïmoud, Y. Feng and J. Liu, *An efficient and accurate hybrid method for simulating non-linear neutrino structure*, *Mon. Not. Roy. Astron. Soc.* **481** (2018) 1486 [[1803.09854](#)].
- [40] J. Dakin, J. Brandbyge, S. Hannestad, T. Haugbølle and T. Tram, *ν CONCEPT: cosmological neutrino simulations from the non-linear Boltzmann hierarchy*, *JCAP* **2019** (2019) 052 [[1712.03944](#)].
- [41] S. Bird, M. Viel and M. G. Haehnelt, *Massive neutrinos and the non-linear matter power spectrum*, *Mon. Not. Roy. Astron. Soc.* **420** (2012) 2551 [[1109.4416](#)].
- [42] F. Villaescusa-Navarro, F. Marulli, M. Viel, E. Branchini, E. Castorina, E. Sefusatti et al., *Cosmology with massive neutrinos I: towards a realistic modeling of the relation between matter, haloes and galaxies*, *Journal of Cosmology and Astro-Particle Physics* **2014** (2014) 011 [[1311.0866](#)].
- [43] E. Castorina, E. Sefusatti, R. K. Sheth, F. Villaescusa-Navarro and M. Viel, *Cosmology with massive neutrinos II: on the universality of the halo mass function and bias*, *JCAP* **2014** (2014) 049 [[1311.1212](#)].
- [44] J. Wang and S. D. M. White, *Discreteness effects in simulations of hot/warm dark matter*, *Mon. Not. Roy. Astron. Soc.* **380** (2007) 93 [[astro-ph/0702575](#)].
- [45] J. Brandbyge and S. Hannestad, *Grid based linear neutrino perturbations in cosmological N-body simulations*, *Journal of Cosmology and Astro-Particle Physics* **2009** (2009) 002 [[0812.3149](#)].
- [46] Y. Ali-Haïmoud and S. Bird, *An efficient implementation of massive neutrinos in non-linear structure formation simulations*, *Mon. Not. Roy. Astron. Soc.* **428** (2013) 3375 [[1209.0461](#)].
- [47] M. Viel, M. G. Haehnelt and V. Springel, *Inferring the dark matter power spectrum from the Lyman α forest in high-resolution QSO absorption spectra*, *Mon. Not. Roy. Astron. Soc.* **354** (2004) 684 [[astro-ph/0404600](#)].

- [48] K. K. Rogers, S. Bird, H. V. Peiris, A. Pontzen, A. Font-Ribera and B. Leistedt, *Simulating the effect of high column density absorbers on the one-dimensional Lyman α forest flux power spectrum*, *Mon. Not. Roy. Astron. Soc.* **474** (2018) 3032 [[1706.08532](#)].
- [49] K. K. Rogers, S. Bird, H. V. Peiris, A. Pontzen, A. Font-Ribera and B. Leistedt, *Correlations in the three-dimensional Lyman-alpha forest contaminated by high column density absorbers*, *Mon. Not. Roy. Astron. Soc.* **476** (2018) 3716 [[1711.06275](#)].
- [50] S. Chabanier, N. Palanque-Delabrouille, C. Yèche, J.-M. Le Goff, E. Armengaud, J. Bautista et al., *The one-dimensional power spectrum from the SDSS DR14 Ly α forests*, *JCAP* **2019** (2019) 017 [[1812.03554](#)].
- [51] A. Font-Ribera, P. McDonald and A. Slosar, *How to estimate the 3d power spectrum of the Lyman- α forest*, *Journal of Cosmology and Astroparticle Physics* **2018** (2018) 003ã003.
- [52] L. Hui and N. Y. Gnedin, *Equation of state of the photoionized intergalactic medium*, *Mon. Not. Roy. Astron. Soc.* **292** (1997) 27 [[astro-ph/9612232](#)].
- [53] Z. Lukić, C. W. Stark, P. Nugent, M. White, A. A. Meiksin and A. Almgren, *The Lyman α forest in optically thin hydrodynamical simulations*, *Mon. Not. Roy. Astron. Soc.* **446** (2015) 3697 [[1406.6361](#)].
- [54] N. Palanque-Delabrouille, C. Yèche, A. Borde, J.-M. Le Goff, G. Rossi, M. Viel et al., *The one-dimensional Ly α forest power spectrum from BOSS*, *Astron. Astrophys.* **559** (2013) A85 [[1306.5896](#)].
- [55] V. Iršič, M. Viel, T. A. M. Berg, V. D’Odorico, M. G. Haehnelt, S. Cristiani et al., *The Lyman α forest power spectrum from the XQ-100 Legacy Survey*, *Mon. Not. Roy. Astron. Soc.* **466** (2017) 4332 [[1702.01761](#)].